



**HAL**  
open science

## Actuator Fault Tolerant System For Cryogenic Combustion Bench Cooling Circuit

Camille Sarotte, J. Marzat, H el ene Piet Lahanier, Alessandra Iannetti, Marco  
Galeotta, G erard Ordonneau

► **To cite this version:**

Camille Sarotte, J. Marzat, H el ene Piet Lahanier, Alessandra Iannetti, Marco Galeotta, et al.. Actuator Fault Tolerant System For Cryogenic Combustion Bench Cooling Circuit. IFAC-PapersOnLine, 2018, 51 (24), pp.592-599. 10.1016/j.ifacol.2018.09.636 . hal-02475680

**HAL Id: hal-02475680**

**<https://hal.science/hal-02475680>**

Submitted on 12 Feb 2020

**HAL** is a multi-disciplinary open access archive for the deposit and dissemination of scientific research documents, whether they are published or not. The documents may come from teaching and research institutions in France or abroad, or from public or private research centers.

L'archive ouverte pluridisciplinaire **HAL**, est destin ee au d ep ot et  a la diffusion de documents scientifiques de niveau recherche, publi es ou non,  emanant des  tablissements d'enseignement et de recherche fran ais ou  trangers, des laboratoires publics ou priv es.

# Actuator Fault Tolerant System For Cryogenic Combustion Bench Cooling Circuit

C. Sarotte\* J. Marzat\* H. Piet Lahanier\* A. Iannetti\*\*  
M. Galeotta\*\* G. Ordonneau\*

\* DTIS, ONERA, Université Paris-Saclay, F-91123 Palaiseau, France

\*\* CNES, Paris, France

---

**Abstract:** In this paper a method is proposed to design a fault tolerant control strategy based on a pressure and mass flow rate model, as well as a fault detection and isolation scheme to improve the reliability of a cryogenic bench operation. The fault is detected by the fault detection and isolation scheme composed of an extended unknown input observer, a cumulative sum algorithm and an exponentially moving average chart. Then the goal is to provide a fault tolerant system reconfiguration mechanism with a control law which compensates for the estimated actuator additive faults to maintain the overall system stability. For that purpose we use a linear quadratic regulator on an equivalent system where the unknown input is expressed as a function of the known state and known input vectors. The model and the estimation part were validated on the real Mascotte test bench (ONERA/CNES) data, and the reconfiguration control law was validated in realistic simulations.

*Keywords:* Change detection, actuator fault accommodation, cryogenic system, fault tolerant control, fault detection and isolation

---

## 1. INTRODUCTION

The need for increased launch safety and launcher's engines reliability leads to the development of health monitoring systems. The experience acquired during the years of Ariane 5 system's exploitation has pointed out the complexity of the implementation of cryogenic propulsive systems as well as the necessity to get a specialized expertise on physical phenomenon. In terms of traditional engines the objective is the improvement and the reliability of the implementation (see Iannetti et al. (2014)). It is then necessary to be able to handle emergency situations arising from actuator failures that can affect the engine performance. The failure should be detected quickly, then isolated and its causes should be identified. For that purpose, Fault detection and isolation (FDI) methods have been developed to evaluate failures and take a decision using all available information with the help of explicit or implicit models. The most common model-based approach makes use of observers to generate residuals. Faults are detected by setting a fixed or variable threshold on each residual signal as in Basseville et al. (1993). Those FDI methods assume that the mathematical model used is representative of the system dynamics. This is challenging in practice because of the presence of modeling uncertainties and unknown disturbances. To tackle the problem of those unknown disturbances, a simple class of full order observers for linear systems with unknown inputs. It consists in a coordinate system transformation that decouples the disturbance effect on the system outputs. The observer resulting from such an approach is called Unknown input observer (UIO) (see for example Darouach et al. (1994)). An UIO is used to estimate the unknown state of the

system independently of the unknown input. In the case of non-linear systems one of the developed techniques is to linearize and design an Extended unknown input observer (EUIO) as described in Witczak (2007).

Once the fault is detected by the FDI method based on observers, one solution to accommodate the presence of fault is to adopt a Fault tolerant control (FTC) strategy, for example see Cieslak et al. (2008); Hamayun et al. (2013). The main objective of a Fault tolerant control system (FTCS) is to maintain, with a control reconfiguration mechanism, current performances close to the desirable ones and preserve stability conditions in the presence of component and/or instrument faults. An active FTCS is characterized by an on-line FDI process (Zhang and Jiang (2008)) which detects and estimates the fault, the second step is to achieve a steady-state tracking of the reference input by compensating the fault (Theilliol et al. (2008)). In this paper a FTC method for the cooling circuit of a cryogenic combustion bench, Mascotte (CNES/ONERA), is studied. This bench has been developed to study heat transfers in the combustion chamber and jet separation in nozzles in the same conditions as for Vulcain 2 motor. The method proposed here is based on a physical model giving the output pressure and mass flow rate of the cooling circuit (Section 2). This model presenting non-linearity and unknown terms is more complete than the previous one established in Iannetti et al. (2014). To generate residuals we estimate the state with the help of an EUIO (Section 3) and reconstruct the unknown input with the help of a high order sliding modes observer proposed by Kalsi et al. (2010); Zhu (2012). Then the residual is analyzed with a Cumulative sum (CUSUM) algorithm using an Exponentially weighted moving average (EWMA-C) chart

to detect a mean shift (Jiang et al. (2008); Ryu et al. (2010); Basseville et al. (1993)). If an actuator failure is detected we switch to a FTCS (Section 4) to design a controller based on an unknown input observer by considering the fault to be the unknown input similar to Hamayun et al. (2013). This complete FDI/FTC loop permits to localize an actuator fault thanks to an estimation of the full state in spite of unmeasured information and then to compensate on-line for the fault. The results are obtained with off-line tests based on real experimental data and the reconfiguration control law was validated on realistic simulations based on the established model.

## 2. SYSTEM DESCRIPTION

The cryogenic combustion bench Mascotte (Figure 1) performs an oxygen / hydrogen operation with pressures and mass flow rates comparable to an injection element of the Vulcain 2 engine. The system studied here is its water cooling circuit. This part of the circuit feeds the combustion chamber. The detection of a leak or an obstruction is a critical safety task for the bench operation. The water cooling circuit consists in different pipes sections with multiple pressure release valves and a tank at the inlet. The available measurements are pressure, mass flow and temperature. Sections are separated by sliding valves with additional pressure measurements.

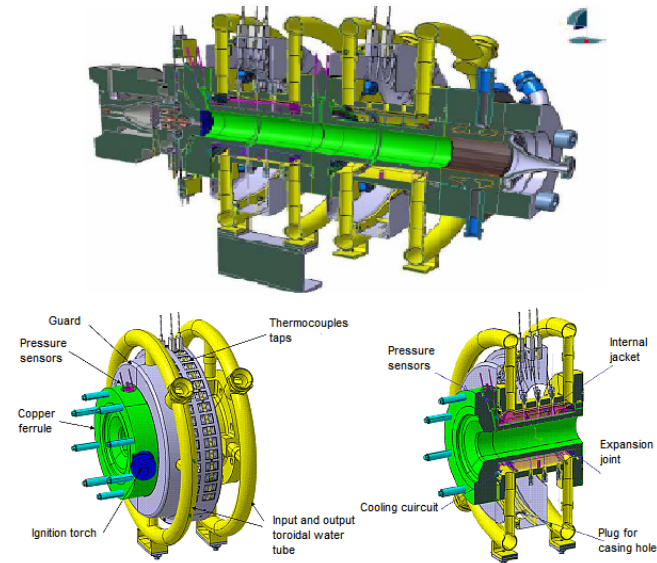


Fig. 1. Mascotte test bench - Ferrules (ONERA - CNES)

The circuit between two ferrules can be modeled by two cavities defined in pressure and temperature linked by an orifice where friction forces and heat flux exchanges are taken into account, see Iannetti et al. (2014). A pressure regulator (actuator) permits to regulate the first cavity pressure of the water cooling circuit.

The method used here (Figure 2) consists of a loop composed of a first EUIO (unknown output mass flow rate) for fault detection purpose and another loop with a second EUIO (actuator failure) for FTC purpose. Once and only if a change has been detected by the FDI function, the

FTC is included in the closed-loop system. The fault estimate is calculated from the estimated unknown mean shift provided by the ACUSUM. Then the second EUIO ensures the estimation error convergence (and stability) and the feedback controller ensures the reconfiguration error convergence (and stability).

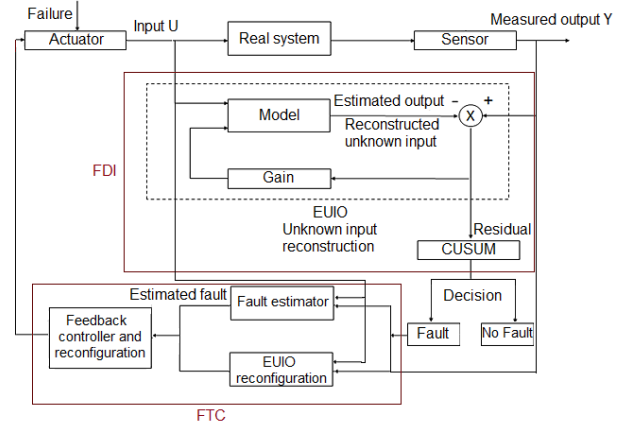


Fig. 2. Diagram of the complete loop

The performances of the algorithms are evaluated by two means. The first one is based on off-line tests realized with real measurements of the project Conforth (CNES/ONERA). During those trials, pressures (cavities 1 and 2), temperatures (cavities 1, 2 and wall) and output mass flow rate have been recorded. The second one is based on a simulator, Carins (CNES/ONERA). This simulator permits to simulate failures for the evaluation of performances with various faults.

### 2.1 Model of the cooling circuit

In this section we denote  $\dot{m}$  the mass flow rate (kg/s),  $\rho$  the density (kg/m<sup>3</sup>),  $S$  the surface (m),  $c$  the velocity of sound (m/s),  $u$  the fluid velocity (m/s),  $P$  the pressure (Pa),  $D$  the orifice diameter (m),  $D_h$  the hydraulic diameter (m),  $L$  the length (m),  $r$  the radius (m),  $\mu$  the dynamic viscosity (Pa.s) and  $V$  the volume (m<sup>3</sup>),  $d_t$  the time step (s).

The flow is assumed to stay monophasic, is ideal (no force due to viscosity acts) and incompressible following Euler equations. The cavity section is assumed constant and the velocity of sound is defined as for an isentropic reaction in the orifice. We assume that the fluid flow velocity is small in comparison to the velocity of sound.

The flow crossing cavities respects the mass balance equation, after integrating this equation along the cavity length, we obtain:

$$\frac{\partial P}{\partial t} = \frac{c^2}{V}(\dot{m}_e - \dot{m}_s) \quad (1)$$

The flow crossing the orifice between the two cavities respects the momentum balance equation with friction forces, expressed with the Darcy-Weisbach and Blasius equations for moderate turbulent flows in a smooth pipe (Nakayama (1998)). After integrating this equation along the orifice length we obtain:

$$\frac{1}{S^2} \frac{\partial \dot{m}}{\partial t} + \frac{\Delta P}{V} = -0.316 \left( \frac{4\dot{m}}{\pi D \mu} \right)^{-\frac{1}{4}} \frac{L}{D_h} \frac{\dot{m}^2}{2\rho V S^2} \quad (2)$$

The model of this part of the cooling circuit is then:

$$\begin{cases} \frac{\partial \dot{m}_{2e}}{\partial t} = \theta_1 \dot{m}_{2e}^{\frac{7}{4}} - \theta_2 \Delta P \\ \frac{\partial P_2}{\partial t} = -\theta_3 \Delta \dot{m} \end{cases} \quad (3)$$

$$\theta_1 := -0.316 \left( \frac{4}{\pi D \mu} \right)^{-\frac{1}{4}} \frac{L}{D_h} \frac{1}{2\rho V}$$

$$\theta_2 := \frac{S^2}{V}, \theta_3 := \frac{c^2}{V}$$

The parameter  $\theta_1$  must be identified since the distance  $L$  is unknown. We can assume here that the density and the viscosity remain constant for the considered pressures and temperature ranges. A first model of the cooling circuit has been proposed in Iannetti et al. (2014) with a constant mass flow rate.

This model (Model 1) presented approximations in the transient of the test bench inducing the presence of a pressure difference square root (see Figure 3). Moreover the mass flow rate dynamics was not modeled. The model (Model 2) presented here permits to determine the pressure but also the mass flow rate and it is now possible to model their evolution during the motor speed transients. The model was tested off-line with real measurements of the project Conforth as inputs. Those trials last 60 seconds. The final evolution of the pressure dynamics is well reconstituted (Table 1).

Table 1. Relative errors of the pressure model 1 and 2

Model	Total (%)	Transient (%)	Permanent (%)
Pressure (1)	10.58	13.35	5.04
Pressure (2)	5.44	8.01	0.31
Input mass flow rate (2)	3.31e-5	4.97e-5	6.17e-8

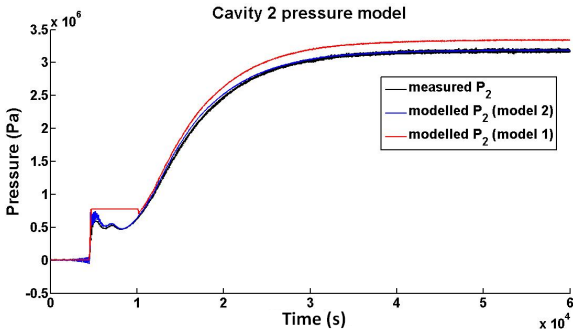


Fig. 3. Pressure model - Project Conforth - Real data

## 2.2 Parameter identification

One way to identify  $\theta_1$  is to use recursive least-squares by selecting one steady-state equilibrium point for the mass flow rate and the pressures. An alternative used here is

the Hagen-Poiseuille formula (Nakayama (1998)) in one steady-state equilibrium point for the mass flow rate and the pressures to express the unknown length as a function of the average mass flow rate  $\dot{m}_{av}$ :

$$L = -\frac{\rho S}{32\mu} \frac{\Delta P}{\dot{m}_{av}} D^2 \quad (4)$$

Finally,

$$\theta_1 := 0.316 \left( \frac{4}{\pi D \mu} \right)^{-\frac{1}{4}} \frac{SD\Delta P}{64V\mu\dot{m}_{av}}$$

For a circular pipe the hydraulic diameter  $D_h$  is equal to the pipe diameter.

The set of parameters is chosen in order to fit with the measurements and in accordance with the known geometric properties of the test bench (see Table 2). Since Carins simulations and the Project Conforth do not have the same pressure reference, the parameter  $\theta_1$  varies.

Table 2. Parameters for estimation and control

Parameters	Carins	Mascotte - Conforth
$\theta_1$	-0.1858	-0.2864
$\theta_2$	6.07	6.07
$\theta_3$	2.25	2.25

## 3. FAULT DETECTION AND ISOLATION

### 3.1 Unknown Input Observer design

The first step is to design an observer to estimate the state in the presence of unknown inputs. The system (3), can be rewritten as a linear time-varying system with an unknown input by linearizing around a steady-state equilibrium trajectory corresponding to the mass flow trajectory to estimate the engine speed transients. Then, the system can be transformed into an equivalent discrete-time state space system with an Euler explicit scheme:

$$\begin{cases} X_{k+1} = A_k(\bar{X})X_k + BU_k + ED_k \\ Y_{k+1} = CX_{k+1} \end{cases} \quad (5)$$

where  $X_k$  is the state vector,  $Y_k$  is the measured output vector,  $U_k$  is the known measured input vector,  $D_k$  is the unknown input vector and  $\bar{X}$  is the equilibrium state.

$$X_k := \begin{bmatrix} \dot{m}_{2e,k} \\ P_{2,k} \end{bmatrix}, Y_k := P_{2,k}, U_k := P_{1,k}, D_k := \dot{m}_{2s,k}$$

Where  $\dot{m}_{2e}$  is the cavity 2 input mass flow rate,  $P_2$  is the cavity 2 pressure,  $P_1$  is the cavity 1 pressure and  $\dot{m}_{2s}$  is the cavity 2 unknown output mass flow rate.

With  $A_k$  the state matrix,  $B$  the known input distribution matrix,  $E$  the unknown input distribution matrix and  $C$  the output distribution matrix.

$$A_k := \begin{bmatrix} 1 + d_t \frac{7\theta_1 \dot{m}_{2e,k}^{\frac{3}{4}}}{4} & -d_t \theta_2 \\ d_t \theta_3 & 1 \end{bmatrix}$$

$$B := [d_t \theta_2 \ 0]^T$$

$$E := [0 \ -d_t \theta_3]^T$$

$$C := [0 \ 1]$$

The first objective is to design an observer depending only on known input and output measurements. We propose to use an EUIO with the following structure (Witczak (2007)):

$$\begin{cases} Z_{k+1} = N_{k+1}Z_k + K_{k+1}Y_k + GU_k \\ \hat{X}_{k+1} = Z_{k+1} + HY_{k+1} \end{cases} \quad (6)$$

The above matrices are designed in such a way as to ensure unknown input decoupling as well as the minimization of the state estimate error.

$$e_k = \hat{X}_k - X_k = Z_k - X_k + HY_k \quad (7)$$

To reduce its expression to a homogeneous equation we impose:

$$G = TB \quad (8)$$

$$TA_k - N_{k+1}T - K_{k+1}C = 0 \quad (9)$$

$$TE = 0 \quad (10)$$

With  $T = I_n - HC$  and  $n$  the dimension of the state.

A necessary condition for the existence of a solution is  $\text{rank}(CE) = \text{rank}(E)$ . A particular solution is then:

$$H = E((CE)^T(CE))^{-1}(CE)^T \quad (11)$$

The matrix  $N_{k+1}$  should be Hurwitz to make the observer converge asymptotically.

This is the case if we choose:

$$N_{k+1} = TA_k - K_{k+1}C \quad (12)$$

The gain matrix  $K_{k+1}$  is chosen to minimize the variance of the state estimation error. For a linear estimator under gaussian hypotheses (the standard deviation is denoted  $\sigma$ ), this translates into:

$$K_{k+1} = TA_{k+1}P_kC^T(C_kP_kC^T - R_k)^{-1} \quad (13)$$

The covariance matrix is then given by:

$$\begin{aligned} P_{k+1} &= TA_{k+1}P_kTA_{k+1}^T - K_{k+1}CP_kTA_{k+1}^T \\ &+ HR_{k+1}H^T + TQ_kT^T \end{aligned} \quad (14)$$

The estimation cadence used on real measurements of the project Conforth is fixed to 0.03 second, the acquisition machine acquires one point each 0.01 second and delivers information to the surveillance machine at a rate of one point each 0.03 second. The state estimation error (7) is taken as a residual.

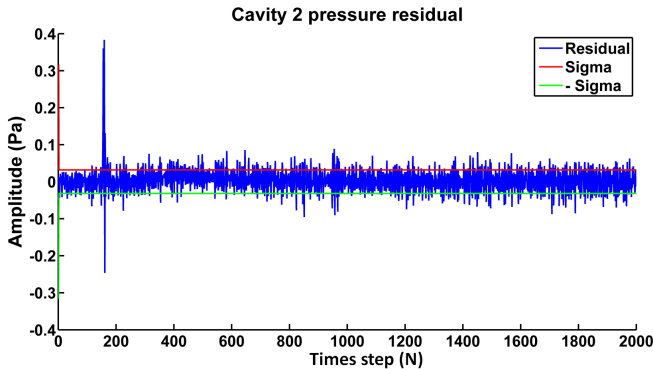


Fig. 4. Pressure residual - Project Conforth

Table 3. Relative errors of the pressure and input mass flow rate estimations

Model	Total (%)	Transient (%)	Permanent (%)
Pressure (Pa)	9.92e-2	7.00e-2	1.16e-2
Mass flow rate (kg/s)	6.27	31.4	1.18e-2

Figure 4 and Table 3 report the estimation results of the UIO, which are very satisfactory. Moreover in the case where it is not possible to measure the mass flow rates we can obtain an accurate estimate, in the permanent regime of the engine. The first peak in Figure 4 corresponds to the transient.

### 3.2 FDI with an adaptive CUSUM and EWMA-C shift estimator

The FDI mechanism is supposed to detect and diagnose any relevant failure that could lead to engine performance degradations. This shall be done sufficiently early to set up timely safe recovery. One way to proceed to detect faults is to evaluate the residual corresponding to our state estimator error. The objective is then to be able to detect a residual mean shift for a nominal behavior, see Basseville et al. (1993).

The two hypotheses considered are then:

H0: The mean value of the residual is nominal  $\mu = \mu_0$

H1: The mean value of the residual has a shift  $\mu = \mu_1$

In most common practical cases  $\mu_1$  is unknown. This can be overcome by using Adaptive CUSUM algorithm (ACUSUM) which estimates this value as in Jiang et al. (2008).

As mean shift amplitudes can vary drastically for a class of failure, the estimator designed for  $\delta$  is a generalization of the Exponentially Weighted Moving Average (EWMA) which presents enhanced efficiency for estimation of large mean shifts:

$$\hat{\delta}_k = \hat{\delta}_{k-1} + \Phi_\gamma(e_{p,k}) \quad (15)$$

With  $e_{p,k} = r_k - \hat{\delta}_{k-1}$  the prediction error,  $\Phi_\gamma$  is defined as a Huber score function.

$$\Phi_\gamma := \begin{cases} e_p + (1 - \lambda)\gamma, & e_p < -\gamma \\ \lambda e_p, & |e_p| \leq \gamma \\ e_p - (1 - \lambda)\gamma, & e_p > \gamma \end{cases}$$

With  $\gamma \geq 0$ , usually fixed constant.

This leads to the following ACUSUM Statistic:

$$s_k = \frac{\pm |\hat{\delta}_\pm|}{\sigma^2} \left( r_k - \mu_0 \pm \frac{|\hat{\delta}_\pm|}{2} \right) \quad (16)$$

where for a mean shift increase or decrease:

$$\hat{\delta}_+ := \max(\delta_{+,min}, \hat{\delta}_k), \quad \hat{\delta}_- := \min(\delta_{-,min}, \hat{\delta}_k)$$

$\delta_{+,min}$  and  $\delta_{-,min}$  are here the minimum mean shifts amplitudes to detect.

The threshold is chosen to be a security coefficient times  $\hat{\delta}_+$  (Table 4).

Table 4. Parameters for fault detection

Parameters	Values
$\delta_{+,min}$	4e-2
$\delta_{-,min}$	-4e-2
$\lambda$	1.1055
Threshold coefficient	4.5e4

$\gamma$  is defined here at each step by  $\gamma := |r_k - \hat{\delta}_{k-1}| / 2$ .

With this choice of  $\gamma$ , the algorithm is more efficient for the detection of small shifts. This generalization is referred to as an EWMA-C statistic. To select the coefficients values and test the algorithm performance, three faults have been simulated with Carins for different profiles of the cooling circuit inflow valves closures and openings. The objective of this FDI system is to be able to detect abrupt changes and to differentiate state perturbations and speed transients characterized by slower variations from a failure.

The first fault simulated is abrupt with a large mean shift (Figure 5), the second one has a slow variation with also a large mean shift (Figure 6) and the third one contains two faults one with a small mean shift, another one with a large mean shift (Figure 7). The first one has a slow shift then an abrupt recovery; the second one has an abrupt shift and a slow recovery. The total time of the simulation is 60 seconds with a time step of 1 millisecond (Table 5). The cadence of the estimation and the detection is 1 time step per 30 milliseconds.

Table 5. Simulated faults

Fault	$t_{begin}(s)$	$t_{end}(s)$	$N_{begin}$	$N_{end}$
Fault 1	41010	46200	1367	1540
Fault 2	30960	37560	1032	1252
Fault 3(1)	39300	41040	1310	1368
Fault 3(2)	45960	60000	1532	2000

The EUIO from the previous subsection permits to estimate outputs and generate the residual as the state estimator error defined by  $r_k := Y_k - C\hat{X}_k$ .

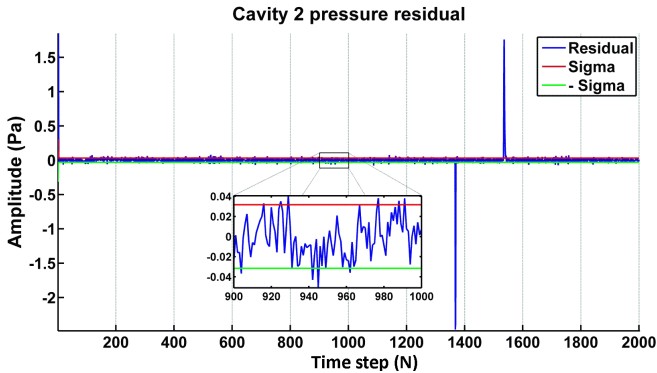


Fig. 5. Fault 1 residual - Carins simulation

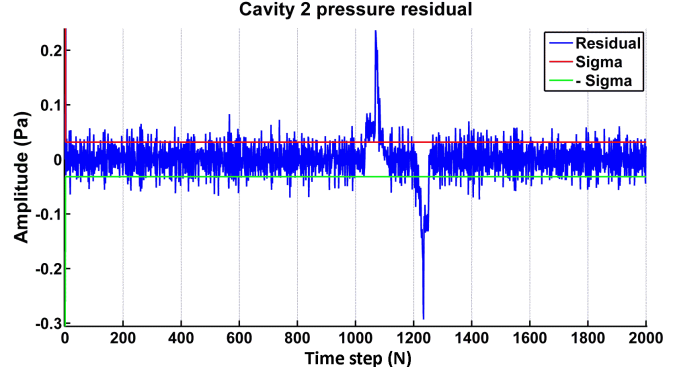


Fig. 6. Fault 2 residual - Carins simulation timespan

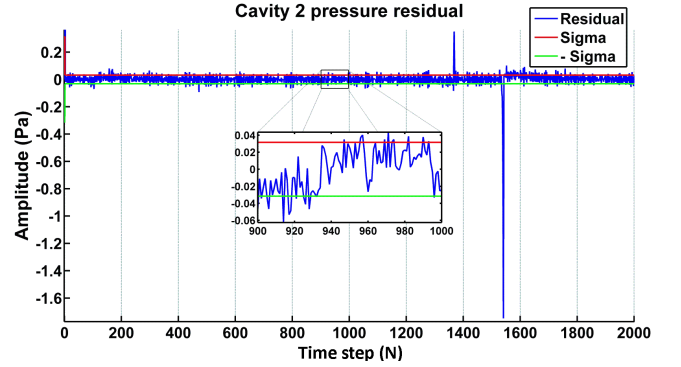


Fig. 7. Fault 3 residual - Carins simulation

After eliminating the effect of process input signals, filtering the effect of disturbances and model uncertainties on the residual, a residual evaluator has been designed by choosing an evaluation function and determining the threshold. To evaluate the effectiveness of the designed algorithm, the good detection (GDR) and false detection rates (FDR) have been calculated.

The good detection rate (GDR) is defined as:

$$GDR := 100.N_{GD}/\Delta t_{fault}$$

and, the false detection rate (FDR) is defined as:

$$FDR := 100.N_{FD}/(\Delta t_{detection} - \Delta t_{fault})$$

with  $N_{GD}$  the number of good detection,  $N_{FD}$  the number of false detection,  $\Delta t_{fault}$  the fault timespan and  $\Delta t_{detection}$  the detection timespan.

Table 6. Detection rates

Fault	GDR	FDR
Fault 1	98.8%	0.0%
Fault 2	27.4%	0.0%
Fault 3	98.5%	14.5%

Those rates have been calculated from ten runs for each simulation and the settings have been chosen to optimize the good detection rate and minimize the false detection rate of abrupt mean shifts. Results on Fault 2 are satisfactory since it is not mandatory to detect slow variations that can be confused with transients (see Table 6). Good

results are obtained for Faults 1 and 3. The last case permits to evaluate the algorithm performance for successive faults of different sizes and this is better to avoid false alarms. In some rare cases the system behavior between two faults can be considered to be faulty but in most cases the two faults in Fault 3 are well detected.

#### 4. ACTIVE FTCS FOR THE INPUT PRESSURE

We consider in this part an additive actuator failure on the system. Once the fault has been detected by an on-line and real-time FDI mechanism the goal is to maintain the overall system stability and an acceptable performance in spite of the occurrence of faults by reconfiguring the nominal control law.

Since the system is controllable in pressure and a pressure failure induces a mass flow rate failure, it is necessary to be able to decouple the fault effect on the system dynamics from the unknown input one. The first step is then to decouple the reconstructed cavity 2 output mass flow rate from the system dynamics in order to evaluate the actuator fault and compensate it.

This method can also be useful in the case of Vulcain 2 engine during an Ariane flight, where it is difficult or expensive to measure the mass flow rate.

##### 4.1 Unknown Input Reconstruction via high order observer

In Zhu (2012) and Kalsi et al. (2010), an auxiliary output vector is introduced so that the observer matching condition is satisfied and is used as the new system output to asymptotically estimate the system state without suffering the influence of the unknown inputs. From this result, it is possible to build an unknown input reconstruction method based on both the state and the auxiliary output derivative estimates.

The auxiliary output is defined as:

$$Y_{a,k}^i := C_{a,k}^i X_k$$

with  $i = 1, \dots, p$  and  $p$  is the number of rows of  $Y_k$ .

The auxiliary output vector contains the output information of the original system.

If we denote:

$$C_{a,k} := [C_1 \dots C_1 A_k^{\gamma_1-1} \dots C_p \dots C_p A_k^{\gamma_p-1}]^T$$

with  $1 \leq \gamma_i \leq n_i$   $i = 1, \dots, p$  where  $n_i$  is defined as the smallest integer such that:

$$\begin{cases} c_i A_k^{\gamma_i} E = 0 & \gamma_i = 0, 1, \dots, n_i - 2 \\ c_i A_k^{n_i-1} E \neq 0 \end{cases} \quad (17)$$

and  $C_i$  the  $i$ -th row of  $C$ .

$$C_{a,k}^i := [C_i \dots C_i A_k^{\gamma_i-1}]^T$$

Since the auxiliary output vector depends on unmeasured variables, we can design a high-order sliding mode observer to get the estimates of both the auxiliary output vector and its derivative.

After discretization we have:

$$Y_{a,k+1}^i = C_{a,k+1}^i (A_k X_k + B U_k + E D_k) \quad (18)$$

If we denote:

$$\Lambda_i := \begin{bmatrix} 0 & I_{\gamma_i-1} \\ 0 & 0 \end{bmatrix}, \quad r_i := \begin{bmatrix} 0_{(\gamma_i-1) \times 1} \\ 1 \end{bmatrix}, \quad \Psi_k^i := C_{a,k}^i B$$

Then (18) can be written as:

$$Y_{a,k+1}^i = \Lambda_i Y_{a,k}^i + r_i f_k^i(X_k, D_k) + \Psi_k^i U_k \quad (19)$$

where

$$f_k^i(X_k, D_k) := C_i A_k^{\gamma_i-1} (A_k X_k + E D_k)$$

The last equation of this  $n_i$  size system is:

$$C_i A_k^{\gamma_i-1} E D_k = Y_{a,k+1}^i - C_i A_k^{\gamma_i-1} (A_k X_k + B U_k) \quad (20)$$

The above  $p$  equations can be unified into a single matrix:

$$M_k D_k = \xi_{k+1} - \tilde{C}_k (A_k X_k + B U_k) \quad (21)$$

if we denote

$$M_k := \tilde{C}_k E$$

$$\tilde{C}_k := [(C_1 A_k^{\gamma_1-1})^T \ (C_2 A_k^{\gamma_2-1})^T \ \dots \ (C_p A_k^{\gamma_p-1})^T]^T$$

$$\xi_{k+1} := [(Y_{a,k+1}^1)^T \ (Y_{a,k+1}^2)^T \ \dots \ (Y_{a,k+1}^p)^T]^T$$

Since  $\text{rank}(M_k) = \text{rank}(C_{a,k} D_k) = \text{rank}(D_k) = q$ ,  $M_k^T M_k$  is invertible because  $M_k$  has full column rank. So the input vector satisfies:

$$D_k = (M_k^T M_k)^{-1} M_k^T (\xi_{k+1} - \tilde{C}_k (A_k X_k + B U_k)) \quad (22)$$

An estimation of it is then:

$$\hat{D}_k = (M_k^T M_k)^{-1} M_k^T (\hat{\xi}_{k+1} - \tilde{C}_k (A_k \hat{X}_k + B U_k)) \quad (23)$$

with

$$\hat{\xi}_{k+1} := \begin{bmatrix} C_1 A_k^{\gamma_1+1} \hat{X}_k + C_1 A_k^{\gamma_1-1} B U_k \\ C_2 A_k^{\gamma_2+1} \hat{X}_k + C_2 A_k^{\gamma_2-1} B U_k \\ \dots \\ C_p A_k^{\gamma_p+1} \hat{X}_k + C_p A_k^{\gamma_p-1} B U_k \end{bmatrix}$$

To validate the result, the unknown input reconstruction is compared to the cavity 2 output mass flow rate measurements available for this trial. Results are reported in Figure 8 and Table 7 and show a correct convergence after the transient phase.

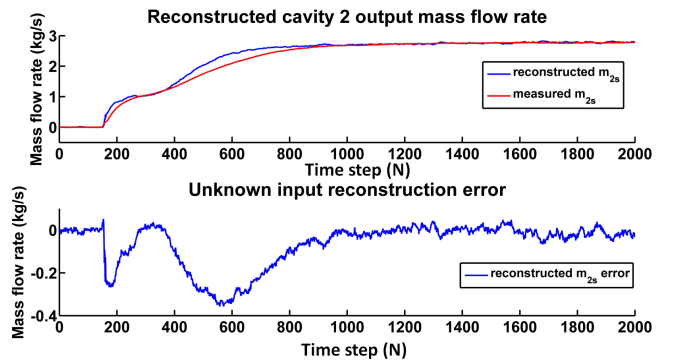


Fig. 8. Unknown input reconstruction - Project Conforth

Table 7. Relative error of the output mass flow rate reconstruction

Model	Total (%)	Transient (%)	Permanent (%)
Output mass flow rate (kg/s)	17.6	35.2	1.19e-2

#### 4.2 Fault tolerant control system design

Now that the unknown input expression is available, we can rewrite the first system without the mass flow rate as an unknown input. Then, in order to annihilate the actuator fault effect on the system, another EUIO is used to estimate the fault magnitude. A control law has then to compensate the fault and be computed such that the faulty system is as close as possible to the nominal one. We can use the previous result (22) from the unknown input reconstruction part to rewrite the system under a second form only depending on known inputs for control purposes:

$$X_{k+1} = AX_k + BU_k + E((M^T M)^{-1} M^T (\xi_{k+1} - \tilde{C}(AX_k + BU_k))) \quad (24)$$

$$X_{k+1} = (I_n - E(M^T M)^{-1} M^T \tilde{C}A)^{-1} [(A - E(M^T M)^{-1} M^T \tilde{C}A)X_k + (B - E(M^T M)^{-1} M^T \tilde{C}B)U_k] \quad (25)$$

The system is linearized around a steady state equilibrium, the nominal state to reach, the matrix  $A$  is then constant in time.

This method requires matrix inversions, which may be numerically unstable due to possible ill-conditioning. In the problem considered, the matrices were invertible.

We obtain a new system under the form:

$$\begin{cases} X_{k+1} = A_c X_k + B_c U_k \\ Y_{k+1} = C X_{k+1} \end{cases} \quad (26)$$

with  $A_c$  the new state matrix and  $B_c$  the new known input distribution matrix:

$$\begin{aligned} A_c &:= (I_n - E(M^T M)^{-1} M^T \tilde{C}A)^{-1} \\ &\quad (A - E((M^T M)^{-1} M^T \tilde{C}A)) \\ B_c &:= (I_n - E(M^T M)^{-1} M^T \tilde{C}A)^{-1} \\ &\quad (B - E((M^T M)^{-1} M^T \tilde{C}B)) \end{aligned}$$

The estimate of the state is given by:

$$\hat{X}_{c,k+1} = \eta_{k+1} + e_{c,k+1} + \bar{X}_{k+1} \quad (27)$$

An additive actuator failure with a control law can be modeled as:

$$\begin{cases} X_{k+1} = A_c X_k + B_c U_{n,k} + B_c (f_k + U_{c,k}) \\ Y_{k+1} = C X_{k+1} \end{cases} \quad (28)$$

where we assume  $U_{n,k}$ , the nominal input, to be known,  $U_{c,k}$  is the control law and  $f_k$  is the faulty part of the input.  $U_{n,k}$  and  $f_k$  are components of  $U_k$ .

It is then possible to design a second unknown input observer for the reconfiguration part, where  $f_k + U_{c,k}$  is considered to be the unknown input, with the following structure (Hamayun et al. (2013)):

$$\begin{cases} Z_{c,k+1} = N_{c,k+1} Z_{c,k} + K_{c,k+1} Y_k \\ \hat{X}_{c,k+1} = Z_{c,k+1} + H_c Y_{k+1} \end{cases} \quad (29)$$

The above matrices are designed in such a way as to ensure unknown input decoupling from the estimation error dynamic as well as the minimization of the state estimator error variance as previously.

$$e_{c,k} = \hat{X}_{c,k} - X_k = Z_{c,k} - X_k + H_c Y_k \quad (30)$$

To reduce this expression to a homogeneous equation we impose:

$$H_c = B_c ((CB_c)^T (CB_c))^{-1} (CB_c)^T \quad (31)$$

$$N_{c,k} = T_c A_c - K_{c,k} C \quad (32)$$

To give the state estimator error the minimum variance, the gain matrix should be determined to minimize the covariance matrix:

$$K_{c,k} = (TA)_c P_k C^T (CP_k C^T - R_k)^{-1} \quad (33)$$

The EUIO stability is addressed in Witczak (2007).

We also have to ensure the convergence of the regulation error  $\eta_k$ .

$$\eta_{k+1} = X_{k+1} - \bar{X}_{k+1} \quad (34)$$

$$\eta_{k+1} = A_c (X_k - \bar{X}_k) + B_c f_k + B_c U_{c,k} \quad (35)$$

$$\eta_{k+1} = A_c \eta_k + B_c f_k + B_c U_{c,k} \quad (36)$$

Then we can use a control law of the form:

$$U_{c,k} := -B_c^+ B_c \hat{f}_k - W_c (\hat{X}_{c,k} - \bar{X}_k)$$

where  $-B_c^+ B_c \hat{f}_k$  is the fault compensation part and  $W_c (\hat{X}_{c,k} - \bar{X}_k)$  is the reconfiguration part. The fault magnitude estimation  $\hat{f}_k$  is obtained from the fault diagnosis part (Section 3.2 Residual) and unknown input reconstruction (Section 4.1 Unknown input estimate). Which can be alternatively written as

$$U_{c,k} := -B_c^+ B_c \hat{f}_k - W_c e_{c,k} - W_c \eta_k$$

Where we denote  $B_c^+$  as the pseudo-inverse of  $B_c$  (Theilliol et al. (2008)). Then we have:

$$\zeta_{k+1} = \begin{bmatrix} A_c - B_c W_c & -B_c W_c \\ 0 & N_c \end{bmatrix} \zeta_k$$

where  $\zeta_k := [\eta_k \ e_{c,k}]^T$ .

For the nominal system, the gain  $W_c$  must stabilize  $(A_c - B_c W_c)$ . Since the pair  $(A_c, B_c)$  is assumed to be controllable, a Linear-Quadratic Regulator (LQR) formulation can be adopted where  $W_c$  is selected to minimize

$$J_k := \sum_k X_k^T Q_{c,k} X_k + U_{c,k}^T R_{c,k} U_{c,k}$$

Where  $Q_{c,k}$  and  $R_{c,k}$  are symmetric positive definite design matrices. It is also possible to proceed to a pole placement for the continuous time system (small time constant), we can choose to fix a damping ratio and a natural frequency.

Table 8. Gain matrix choice

Pressure part	Mass flow rate part	Damping ratio	Natural frequency
-0.3668	-0.9956	2	1e-1

The desired transient behavior depends on the gain choice (Table 8), in our case we have to limit the overshoots to maintain the cooling circuit performances (Figure 9). The fault was implemented as in the previous section. The aim of this simulation is to see if the controller is able to stabilize the closed-loop system after the detection, see Table 9. If a fault is detected then the system switches to the closed-loop one.

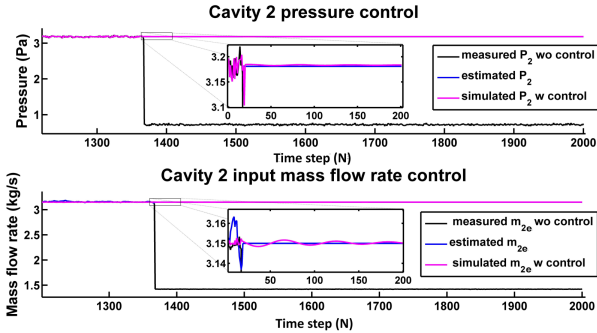


Fig. 9. Pressure and mass flow rate control - Carins simulator - ATAC configuration

When the fault is detected the system switches to the FTCS. The fault is compensated and it can be seen that the control law for the rewritten system permits to stabilize the system around the reference steady-state equilibrium with sufficient precision.

Table 9. Relative errors of the simulated pressure and input mass flow rate from references

Model (2) with control	Permanent (from detection time) (%)
Pressure (Pa)	1.6e-1
Input mass flow rate (kg/s)	7e-2

## 5. CONCLUSION

In this paper a new model was proposed for the evolution of pressure and mass flow rates in the cooling circuit of a cryogenic test bench. Once the fault in the actuator has been detected by the FDI method composed of a first EUIO, the designed FTCS based on a fault estimator and a second EUIO permits to compensate the failure and to converge if necessary to a chosen steady state. This FTCS consist in a linear quadratic regulator on an equivalent system where the unknown input is expressed as a function of the known state and known input vectors in order to decouple only the fault effect on the system. Future work will address the design of a method to calculate another steady point which may be reachable in the case where the previous nominal steady point cannot be reached because of the actuator failure and the effect of the saturation. Being able to choose the nominal behavior of the system may then be useful to take into account actuator saturation.

## REFERENCES

Basseville, M., Nikiforov, I.V., et al. (1993). *Detection of abrupt changes: theory and application*, volume 104. Prentice Hall Englewood Cliffs.

- Cieslak, J., Henry, D., Zolghadri, A., and Goupil, P. (2008). Development of an active fault-tolerant flight control strategy. *Journal of Guidance, Control, and Dynamics*, 31(1), 135–147.
- Darouach, M., Zasadzinski, M., and Xu, S.J. (1994). Full-order observers for linear systems with unknown inputs. *IEEE Transactions on Automatic Control*, 39(3), 606–609.
- Hamayun, M.T., Edwards, C., and Alwi, H. (2013). A fault tolerant control allocation scheme with output integral sliding modes. *Automatica*, 49(6), 1830–1837.
- Iannetti, A., Marzat, J., Piet-Lahanier, H., Ordonneau, G., and Vingert, L. (2014). Development of model-based fault diagnosis algorithms for mascotte cryogenic test bench. In *Journal of Physics: Conference Series*, volume 570, 072006. IOP Publishing.
- Jiang, W., Shu, L., and Apley, D.W. (2008). Adaptive cusum procedures with ewma-based shift estimators. *IIE Transactions*, 40(10), 992–1003.
- Kalsi, K., Lian, J., Hui, S., and Zak, S.H. (2010). Sliding-mode observers for systems with unknown inputs: A high-gain approach. *Automatica*, 46(2), 347–353.
- Nakayama, Y. (1998). *Introduction to fluid mechanics*. Butterworth-Heinemann.
- Ryu, J.H., Wan, H., and Kim, S. (2010). Optimal design of a cusum chart for a mean shift of unknown size. *Journal of Quality Technology*, 42(3), 311.
- Theilliol, D., Join, C., and Zhang, Y. (2008). Actuator fault tolerant control design based on a reconfigurable reference input. *International Journal of Applied Mathematics and Computer Science*, 18(4), 553–560.
- Witczak, M. (2007). *Modelling and estimation strategies for fault diagnosis of non-linear systems: from analytical to soft computing approaches*, volume 354. Springer Science & Business Media.
- Zhang, Y. and Jiang, J. (2008). Bibliographical review on reconfigurable fault-tolerant control systems. *Annual Reviews in Control*, 32(2), 229–252.
- Zhu, F. (2012). State estimation and unknown input reconstruction via both reduced-order and high-order sliding mode observers. *Journal of Process Control*, 22(1), 296–302.